## Spontaneous Lattice Distortion in the Spin-Triplet Superconductor Cu<sub>x</sub>Bi<sub>2</sub>Se<sub>3</sub>

K. Matano, <sup>1,2</sup> S. Takayanagi<sup>®</sup>, <sup>1</sup> K. Ito, <sup>1</sup> S. Nita, <sup>1</sup> M. Yokoyama, <sup>1</sup> M. Mihaescu<sup>®</sup>, <sup>1</sup> H. Nakao, and Guo-qing Zheng, and Guo-qing Zheng <sup>1</sup>Department of Physics, Okayama University, Okayama 700-8530, Japan <sup>2</sup>Department of Physics, Okayama University of Science, Okayama 700-0005, Japan <sup>3</sup>Photon Factory, Institute of Materials Structure Science, High Energy Accelerator Research Organization, Tsukuba 305-0801, Japan

(Received 23 April 2025; revised 25 June 2025; accepted 31 July 2025; published 22 August 2025)

The doped topological insulator Cu<sub>x</sub>Bi<sub>2</sub>Se<sub>3</sub> has attracted considerable attention as a new platform for studying novel properties of spin-triplet and topological superconductivity. In this work, we performed synchrotron x-ray diffraction measurements on  $Cu_xBi_2Se_3$  (0.24 < x < 0.46) to investigate the coupling between the superconducting order parameter and crystal lattice. In the crystals in which the vector order parameter (d vector) is tilted from the crystal high-symmetry directions as evidenced by nematic diamagnetic susceptibility, we find a sizable lattice distortion (~100 ppm) associated with the onset of superconductivity. In contrast, in crystals with the d vector aligned along the high-symmetry directions, we find no appreciable change in lattice constant. Together with a pronounced vestigial behavior of the distortion, the results are clear evidence for an odd-parity  $E_u$  order parameter that couples with trigonal lattice. Furthermore, in the crystal with x = 0.46 where diamagnetic susceptibility is isotropic in the plane, no lattice distortion accompanying the superconducting transition is found, which is in line with a chiral superconducting state in the highly doped region. Our work shows that lattice distortion can be a powerful diagnosing quantity for nematic superconductivity with two-component order parameter.

DOI: 10.1103/ddvn-8c9n

Whether a superconducting transition accompanies a crystal structural change has been a topic of research for long time in spin-singlet superconductors. A volume expansion at the transition into an isotropic superconducting state was discussed already in the early stages of superconductivity research [1]. Later, a spontaneous lattice distortion at the superconducting transition was predicted for heavy Fermion compounds with an anisotropic gap function [2,3]. It was pointed out that the lattice can expand in the directions along which the gap is large [2]. Lattice distortion was also discussed theoretically in cuprate high-temperature superconductors [4], and a volume expansion associated with the superconducting transition was observed experimentally, hinting at a role of phonon coupling [5].

Recently, efforts have been made to turn the topological insulator Bi<sub>2</sub>Se<sub>3</sub>, which has a trigonal primitive lattice belonging to  $D_{3d}$  point group, into a superconductor by doping carriers [6-8]. In the case of Cu<sub>x</sub>Bi<sub>2</sub>Se<sub>3</sub>, nuclear magnetic resonance measurements revealed a broken spinrotation symmetry below  $T_c$  [9], which is a hallmark evidence for spin-triplet superconductivity. Since the inversion symmetry is preserved in this system, the spin-triplet pairing means an odd-parity orbital wave function, thereby establishing Cu<sub>x</sub>Bi<sub>2</sub>Se<sub>3</sub> as a topological superconductor [10,11], which can host gapless conductive states at their boundaries. In particular, quasiparticle excitations, namely, the Majorana zero-energy modes can exist in the vortex core [12,13], which obey non-Abelian statistics and are expected to be applied in fault-tolerant quantum computing [14,15].

The discovery of spin rotation symmetry breaking in Cu<sub>x</sub>Bi<sub>2</sub>Se<sub>3</sub> makes this system an excellent platform for studying the physics of spin-triplet superconductivity, which is much less known compared to spin-singlet cases. It was proposed that the novel state is described by the  $E_{\mu}$ representation with a two-component order parameter [16]. In such case, the order parameter can couple to the trigonal lattice where the in-plane and out-of-plane shear strain tensors transform as the same irreducible representation [17]. Therefore, obtaining experimental evidence for such coupling is crucial for pining down the order parameter in this class of novel superconductors. Previously, it was found that the in-plane nematic Meissner diamagnetism has a symmetry tiled from the crystal high-symmetry directions, which is restored by applying a strong enough magnetic field [18]. The tilting has been interpreted as a consequence of phonon coupling [18], but direct evidence is lacking. Thermal expansion measurements on Nb<sub>x</sub>Bi<sub>2</sub>Se<sub>3</sub> suggest a minute ( $\sim 0.1$  ppm) a-axis change upon the superconducting transition [19], while high-resolution

<sup>\*</sup>Contact author: zheng@psun.phys.okayama-u.ac.jp

x-ray measurements found no distortion in  $Sr_xBi_2Se_3$  [20]. Thus, the coupling between the spin-triplet order parameter and lattice remains unclear, and further investigation is needed.

In this Letter, we report on x-ray diffraction measurements using high-resolution synchrotron light for electrochemically Cu-doped Cu<sub>x</sub>Bi<sub>2</sub>Se<sub>3</sub> characterized by angular-dependent in-plane magnetic susceptibility measurements. We find a spontaneous lattice distortion of the order 100 ppm in crystals with the d vector tilted away from the crystal high-symmetry directions. The distortion starts at a temperature  $T^*$  above  $T_c$  with  $T^* \sim 1.1 \ T_c$ . However, no appreciable distortion was detected in crystals where the d vector aligns along the high-symmetry (axis) directions. Furthermore, for large doping rate (x = 0.46) where the gap is isotropic in the plane, no lattice distortion was found either. These results reveal the novel feature of the coupling between the two component  $E_u$  type superconducting order parameter and trigonal crystal lattice. Our work can also shed light on kagome or iron-based superconductors with two bands and twisted bilayer graphene, where the charge-4e state [21,22] or quadruple fermion state [23] are a focus of study.

Single crystals of Cu<sub>x</sub>Bi<sub>2</sub>Se<sub>3</sub> were prepared by intercalating Cu into Bi<sub>2</sub>Se<sub>3</sub> by the electrochemical doping method described in Refs. [24,25]. First, single crystals of Bi<sub>2</sub>Se<sub>3</sub> were grown by melting stoichiometric mixtures of elemental Bi (99.9999%) and Se (99.999%) at 850 °C for 48 h in sealed evacuated quartz tubes. After melting, the sample was slowly cooled down to 550 °C over 48 h and kept at the same temperature for 24 h. Those melt-grown Bi<sub>2</sub>Se<sub>3</sub> single crystals were cleaved into smaller rectangular pieces of about 14 mg. They were wound by bare copper wire (diameter 0.05 mm), and used as a working electrode. A Cu wire with diameter of 0.5 mm was used both as the counter electrode and the reference electrode. We applied a current of 10 µA in a saturated solution of CuI powder (99.99%) in acetonitrile (CH<sub>3</sub>CN). The obtained crystal samples were then annealed at 560 °C for 1 h in sealed evacuated quartz tubes, and quenched into water. The Cu concentration x was determined from the mass increment of the samples. It is confirmed that the Cu is indeed doped into the crystal by Knight shift measurements which increases with increasing Cu content x [24]. To check the superconducting properties, dc susceptibility measurements were performed using a superconducting quantum interference device with the vibrating sample magnetometer. The angle-dependent in-plane magnetic susceptibility measurements were performed by rotating the sample inside a fixed coil placed in a magnetic field. The angle was determined using two Hall sensors [18]. Synchrotron radiation was employed for the measurements of lattice constants with high resolution. These measurements were performed at the BL-3A beamline of Photon Factory in High Energy Accelerator Research Organization (KEK).

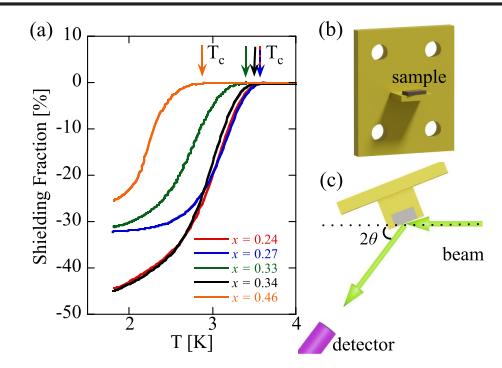


FIG. 1. (a) Results of the dc magnetization measurements for the crystals used in this study. (b),(c) The experimental setup for the synchrotron x-ray diffraction measurements.

The incident beam was monochromatized by a pair of Si(111) crystals. Figure 1(a) shows the results of dc magnetization measurements for the samples used in this study. Figures 1(b) and 1(c) illustrate the experimental setup of the measurements between 1.9 and 12 K. The sample was mounted on a brass holder and measured using a two-axes diffractometer.

First, we present the results for x = 0.24. Figure 2(a) shows the in-plane ac susceptibility as a function of the field angle at T = 1.6 K and H = 0.5 T in the superconducting state [18]. As in the previous reports, a twofold symmetry with an ellipse shape is observed, in which the upper critical field  $H_{c2}$  is the largest along the long axis of the ellipse. The d vector is perpendicular to the long axis of the ellipse [9,18,24], and thus is along the a axis for this crystal. Such nematicity is robust against thermal cycling. As found previously [18,24] and also in this work [26], regardless of x,  $Cu_xBi_2Se_3(x < 0.4)$  can host two kinds of nematic superconducting states with the d vector either parallel or perpendicular to the a axis, which is believed to correspond to the proposed two (almost) degenerate gap functions of  $E_u$  [16]. Figure 2(b) displays the synchrotron diffraction spectrum of (2 2 0) and (3 0 0) reflections. The index (2 2 0) and (3 0 0) correspond to [1 0 0] and [1 1 0] crystal directions. There is no detectable change across  $T_{\rm c}$ . The temperature dependence of the lattice-plane distance  $d_{[100]}$  and  $d_{[110]}$  determined from the peak position is shown in Figs. 2(c) and 2(d), and no difference is seen above and below  $T_c$ .

By contrast, we discover a quite large lattice change in crystals with the d vector tilted away from the high-symmetry direction. Figure 3(a) shows the result for x=0.27. The in-plane magnetic susceptibility exhibited a twofold symmetry, but the long axis of the ellipse is tilted away from the  $a^*$  axis by 5°. Synchrotron diffraction spectra revealed a spectral shift below  $\sim T_c$ , and the directions of the shift are opposite between the [1 0 0] and [1 1 0] direction. The temperature dependence of the lattice-plane distance is shown in Figs. 3(c) and 3(d). The lattice expands along the a-axis direction and contracts

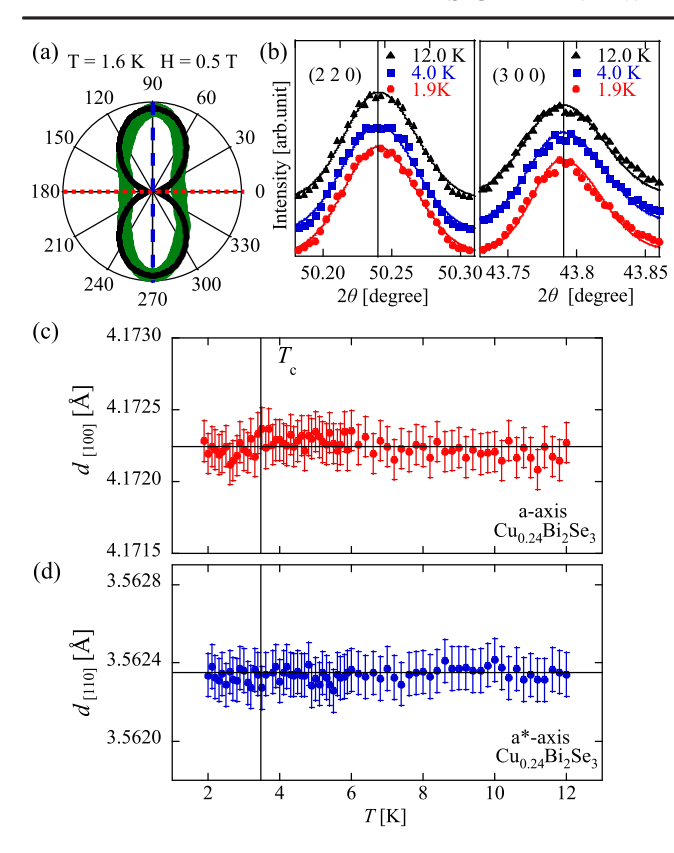


FIG. 2. (a) Diamagnetism measured by in-plane ac susceptibility as a function of the angle  $\phi$  between the predetermined a axis and the applied field. The solid black curve is  $\sin(2\phi)$ . The dotted red and blue line corresponds to the direction along which synchrotron diffraction measurements were performed ([1 0 0] and [1 1 0]), respectively. (b) x-ray diffraction spectrum. The solid curves are fits to two-Gaussian functions. (c),(d) The lattice-plane distance  $d_{[100]}$  calculated from the peak positions at the (2 2 0) and (3 0 0) reflections, respectively. The  $d_{[100]}$  is in agreement with the a-axis constant reported previously [6]. Error bars represent the uncertainties from Gaussian fits.

along the  $a^*$ -axis direction [Figs. 3(c) and 3(d) inset]. We define  $\epsilon = [d(T) - d_0]/d_0$ , the deviation rate of the lattice-plane distance from the value at temperatures well above  $T_c$ , where d(T) represents the value at a temperature T, while  $d_0$  at T=12 K.  $\epsilon$  is found to be 70 ppm in this crystal.

Below, we discuss the origin of the lattice distortion below the superconducting transition. The total free energy of the system at zero magnetic field consists of contributions from the spin-triplet superconducting order which is nematic,  $S_{\text{triplet}}$ , the acoustic phonons (the fluctuations of strain) energy  $S_{\text{phonon}}$ , the coupling between the two,  $S_{\text{triplet-phonon}}$ , and the pinning energy  $S_{\text{pinning}}$  to lock the d vector to a particular direction:

$$S_{\text{total}} = S_{\text{triplet}} + S_{\text{pinning}} + S_{\text{phonon}} + S_{\text{triplet-phonon}}.$$
 (1)

The coupling term is given by [17]

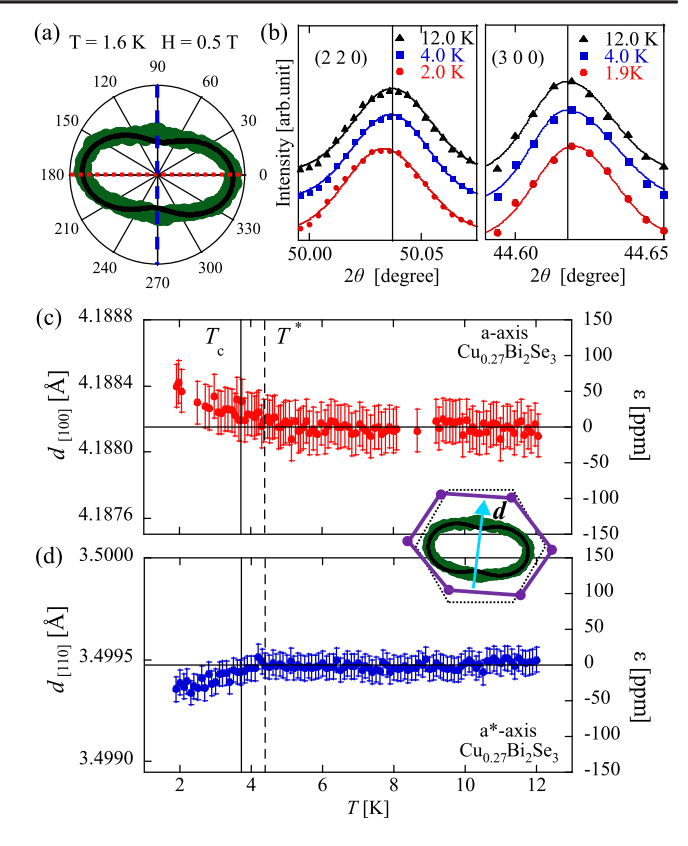


FIG. 3. (a) Angle dependence of the diamagnetism. The solid curve is  $\sin(2\phi+\delta)$ , where  $\delta$  represents the deviation from the high-symmetry direction. (b) Synchrotron x-ray diffraction spectral. (c),(d) The lattice-plane distance  $d_{[100]}$  and  $d_{[110]}$  calculated from the peak positions.  $\epsilon$  is the deviation rate from the value at temperatures well above  $T_{\rm c}$  (see text). The inset shows a schematic illustration of the in-plane crystal distortion. The arrow indicates the d-vector direction.

$$S_{\text{triplet-phonon}} = \int \{ \mathbf{\Psi} \cdot (\kappa_1 \mathbf{e}_1 + \kappa_2 \mathbf{e}_2) \}, \tag{2}$$

where  $\Psi = (\Psi_1, \Psi_2) = (\mathbf{\Delta}^* \boldsymbol{\sigma}^z \mathbf{\Delta}, -\mathbf{\Delta}^* \boldsymbol{\sigma}^x \mathbf{\Delta})$ , with  $\mathbf{\Delta}$  being the two-component spin-triplet nematic order parameter [16] and  $\boldsymbol{\sigma}$  the Pauli matrix.  $\boldsymbol{e}_{1,2}$  is the in-plane shear strain and out-of-plane shear strain doublet, respectively.

$$e_1 = \begin{pmatrix} e_{xx} - e_{yy} \\ -2e_{xy} \end{pmatrix}, \qquad e_2 = \begin{pmatrix} 2e_{yz} \\ -2e_{zx} \end{pmatrix}.$$

The d vector is  $d = \{\Delta_x k_z, \Delta_y k_z, -(v_0/v_z)[\Delta_x k_x + \Delta_y k_y]\}$  [27]. Both  $\Psi$  and  $e_{1,2}$  transform as the same irreducible representation [17], so that they can couple through the nematoelastic coupling constants  $\kappa_1$  and  $\kappa_2$ . This linear coupling mediates the lattice distortion.

The spin-triplet interaction  $S_{\text{triplet}}$  favors the d vector (nematic director) to align parallel to the high-symmetry directions, and the pinning energy  $S_{\text{pinning}}$  is to select one direction among them [18]. The phonon-mediated

interaction prefers the nematic director to align to the directions farthest away from the high-symmetry directions. When the nematoelastic coupling is large enough, it can unlock the nematic director from the high-symmetry directions. Therefore, the tilting of the d vector can be understood as due to a large coupling between  $\Psi$  and  $e_{1,2}$  [18], which can vary from crystal to crystal as the defects in the sample is uncontrollable owing to the quenching process during crystal synthesis. When there are more defects in the sample, acoustic (long wave) phonon propagation could be hindered, resulting in a smaller nematoelastic coupling, whose detailed mechanism needs more investigation in the future though. At any rate, the direct consequence of a large nematoelastic coupling is a large crystal distortion.

Although both the x = 0.24 and x = 0.27 samples exhibit a twofold symmetry at low fields, in the former the *d* vector is oriented along a high-symmetry axis (*a* axis) of the crystal, whereas in the x = 0.27 sample, the **d** vector is tilted away from the  $a^*$ -axis direction, meaning that the nematoelastic coupling is larger in the later. The previously reported results for Sr<sub>x</sub>Bi<sub>2</sub>Se<sub>3</sub> and Nb<sub>r</sub>Bi<sub>2</sub>Se<sub>3</sub> [19,20] can also be well reconciled. The electrical resistivity measurements show that the  $H_{c2}$ shows an ellipselike twofold symmetry with the long axis of the ellipse along the crystal axis. Therefore, the nematoelastic coupling is small there. As a result, the lattice change due to the superconducting transition is expected to be very small, and is indeed in the order of 0.1 ppm as seen in the high-resolution thermal expansion measurement [19] which was unable to be detected by Smylie et al. [20] and in two of our crystals (x = 0.24 and 0.33 [26]) simply because it is beyond the resolution limit of x-ray measurement.

In passing, we note two important properties of the spontaneous lattice distortion. First, the c axis is also distorted [26], therefore the crystal structure is in a triclinic phase under a larger nematoelastic coupling. Second, a close inspection of the data shows that the lattice changes occur at a temperature  $T^*$  slightly above  $T_c$ . Figure 4 plots the values of  $T^*$  against  $T_c$ , including the data for  $Nb_xBi_2Se_3$  [19] and  $Sr_xBi_2Se_3$  where specific heat measurement found an anomaly ascribable to superconductivity above a temperature above the  $T_c$  [28]. A good correlation is seen between  $T^*$  and  $T_c$ . This is another piece of evidence for two-component  $E_u$  order parameter in  $Cu_xBi_2Se_3$  as elaborated below.

A spin-triplet two-component phase is characterized by a  $2 \times 2$  composite order parameter **Q** [27], with the tensor  $\mathbf{Q}_{\alpha\beta} = \sum_{\mu\nu} \boldsymbol{\sigma}_{\mu\nu} \boldsymbol{\sigma}_{\alpha\beta} \Delta^*_{\mu} \Delta_{\nu}$ , where  $\boldsymbol{\sigma} = (\sigma_z, \sigma_x)$ . Explicitly, **Q** can be expressed as

$$\mathbf{Q} = \begin{pmatrix} |\Delta_x|^2 - |\Delta_y|^2 & \Delta_x^* \Delta_y + \Delta_y^* \Delta_x \\ \Delta_x^* \Delta_y + \Delta_y^* \Delta_x & |\Delta_y|^2 - |\Delta_x|^2 \end{pmatrix}. \tag{3}$$

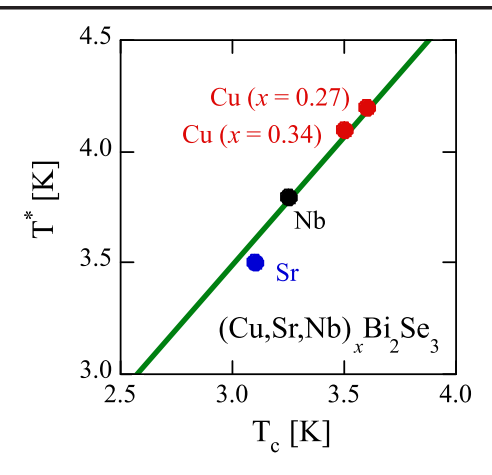


FIG. 4. The precursor temperature  $T^*$  correlated with  $T_c$ . The data point for Sr is from the specific measurement [28], and the data point for Nb is from the thermal expansion measurement [19]. The straight line is a linear fit to  $T^* = kT_c$  with the result k = 1.16.

The expectation value  $\langle \Delta_x \rangle = \langle \Delta_y \rangle = 0$  above  $T_c$ , while the expectation value of  $\mathbf{Q}$  can be finite above  $T_c$ , since  $\langle \Delta_x^* \Delta_y \rangle \neq 0$  for example. As a result, a lattice distortion  $e_{\mu\nu} \propto \kappa \mathbf{Q}_{\mu\nu}$  can develop at a temperature  $T^*$  above  $T_c$ . Therefore, the large discrepancy between  $T_c$  and  $T^*$  by about 15%  $T_c$ , which is not encountered in conventional superconductors where the superconducting-fluctuation temperature range is extremely small and is not accessible by experiments [29], serves as a hallmark for a two-component  $E_u$  superconducting order parameter. We note that the phenomena of charge-4e state [21,22] or quartic fermion phase [23] share similarities with our work in that two components of the order parameter play an essential role.

Finally, Fig. 5 shows the results for x = 0.46. Unlike the results for x < 0.4, the angular dependence of the in-plane magnetic susceptibility yielded an isotropic shape. In synchrotron x-ray diffraction measurements, no changes were observed in the spectra around  $T_c$ . Namely, the lattice constant exhibited no significant change across  $T_c$ . We should first comment on a possible extrinsic cause for the lack of lattice distortion. In the high-doping regime, one may suspect that multiple domains are present which may cause an isotropic in-plane susceptibility and nulls any lattice change. In our synchrotron measurements, the beam size was  $0.05 \times 0.05$  mm<sup>2</sup>. If domains smaller than beam size were present, distortions occurring in different directions would broaden the spectral peaks upon the superconducting transition. However, no such broadening was observed. Therefore, we believe that the observed result is an intrinsic property.

Our previous research has clarified that the symmetry of the superconducting gap changes from nematic to isotropic at around x=0.4 [24]. In angular-dependent measurements of the in-plane upper critical field  $H_{\rm c2}$ , the

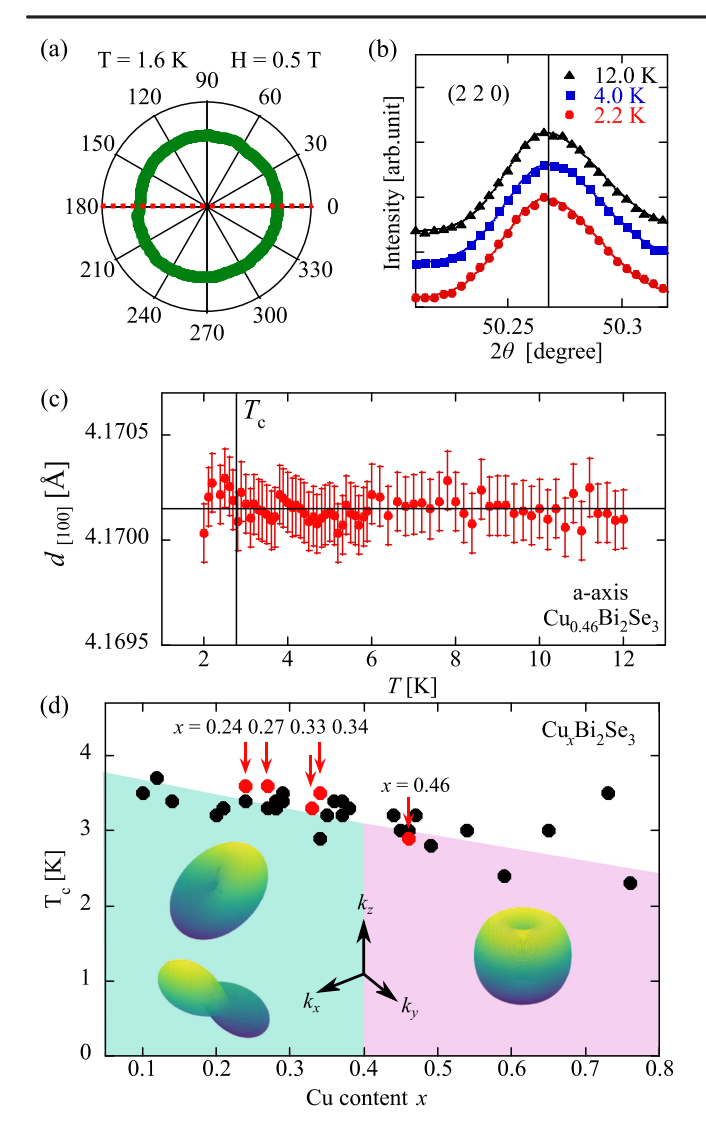


FIG. 5. (a) The in-plane diamagnetism for x = 0.46. (b) Synchrotron x-ray diffraction spectra of the (2 2 0) refection. (c) The lattice-plane distance  $d_{[100]}$  and  $d_{[110]}$  calculated from the peak positions. (d) Cu content x dependence of superconducting critical temperature  $T_{\rm c}$ . The arrows indicate samples measured in this study. The illustrations in each region show the gap functions of the two nematic states and one of the chiral states [16], respectively.

low-doping regime shows twofold symmetry, while the high-doping regime exhibits isotropic behavior. It has been pointed out that [16], the two-component order parameter can result in either a nematic state  $\Delta_x$  or  $\Delta_y$ , or a chiral state in which the gap is isotropic in the hexagonal plane. The gap of the chiral state depends on spin species, one having a full gap and the other nodal gap. Even the later one with two nodes at the poles can be energetically stable as the Fermi surface becomes more two dimensional at higher doping [30]. The synchrotron x-ray diffraction experiments revealing no in-plane distortion accompanying the superconducting transition is consistent with such a chiral superconducting state. Therefore, our new results further

solidify the phase diagram schematically shown in Fig. 5, providing additional supporting evidence for the doping-dependent changes in the pairing symmetry.

In summary, we performed synchrotron x-ray diffraction measurements to investigate whether a lattice distortion occurs at the superconducting transition of the spin-triplet topological superconductor Cu<sub>x</sub>Bi<sub>2</sub>Se<sub>3</sub>. In crystals in which the d vector is tilted from the crystal high-symmetry directions as evidenced by nematic diamagnetic susceptibility, we find a sizable lattice distortion (~100 ppm) associated with the onset of superconductivity. In contrast, in crystals with the d vector aligned along the highsymmetry directions, the lattice distortion is negligibly small. Furthermore, the distortion shows a pronounced vestigial behavior. These results are clear evidence for a two-component order parameter that couples with trigonal lattice. Furthermore, the crystal with x = 0.46 where the gap is isotropic in the plane, no lattice distortion accompanying the superconducting transition is detected, which is in line with a chiral superconducting state in the highly doped region. Our results provide fresh new insights into the physics of superconductivity with two-component oddparity order parameters.

Acknowledgments—We thank R. Fernandes and M. Hecker for stimulating discussions that lead to initiating this work. We are particularly grateful to K. Ishii for coordinating the measurements in KEK. We also thank N. Ikeda and Y. Nogami for helpful discussion on synchrotron light experiments, and A. Kobayashi and S. Kawasaki for participating in the early stage of this project. This work was performed under the approval of the Photon Factory Program Advisory Committee (Proposal No. 2022G657), and supported by KAKENHI (JPSJ Grants No. 22H04482 and No. 25K07207) and the Okayama Foundation for Science and Technology.

Data availability—The data that support the findings of this Letter are not publicly available upon publication because it is not technically feasible and/or the cost of preparing, depositing, and hosting the data would be prohibitive within the terms of this research project. The data are available from the authors upon reasonable request.

<sup>[1]</sup> J. L. Olsen and H. Rohrer, The volume change at the superconducting transition, Helv. Phys. Acta **30**, 49 (1957).

<sup>[2]</sup> R. Joynt and T. M. Rice, Strain distortion in anisotropic superconductors, Phys. Rev. B **32**, 6074 (1985).

<sup>[3]</sup> M.-a. Ozaki, Group theoretical analysis of the lattice distortion in anisotropic superconductivity, Prog. Theor. Phys. 76, 1008 (1986).

<sup>[4]</sup> A. J. Millis and K. M. Rabe, Superconductivity and lattice distortions in high- $T_c$  superconductors. Phys. Rev. B **38**, 8908 (1988).

- [5] H. You, U. Welp, and Y. Fang, Slope discontinuity and fluctuation of lattice expansion near  $T_c$  in untwinned YBa<sub>2</sub>Cu<sub>3</sub>O<sub>7- $\delta$ </sub> single crystals, Phys. Rev. B **43**, 3660 (1991).
- [6] Y. S. Hor, A. J. Williams, J. G. Checkelsky, P. Roushan, J. Seo, Q. Xu, H. W. Zandbergen, A. Yazdani, N. P. Ong, and R. J. Cava, Superconductivity in Cu<sub>x</sub>Bi<sub>2</sub>Se<sub>3</sub> and its implications for pairing in the undoped topological insulator, Phys. Rev. Lett. 104, 057001 (2010).
- [7] Y. Qiu, K. N. Sanders, J. Dai, J. E. Medvedeva, W. Wu, P. Ghaemi, T. Vojta, and Y. S. Hor, Time reversal symmetry breaking superconductivity in topological materials (2015), arXiv:1512.03519.
- [8] Z. Liu, X. Yao, J. Shao, M. Zuo, L. Pi, S. Tan, C. Zhang, and Y. Zhang, Superconductivity with topological surface state in Sr<sub>x</sub>Bi<sub>2</sub>Se<sub>3</sub>, J. Am. Chem. Soc. 137, 10512 (2015).
- [9] K. Matano, M. Kriener, K. Segawa, Y. Ando, and G.-q. Zheng, Spin-rotation symmetry breaking in the superconducting state of Cu<sub>x</sub>Bi<sub>2</sub>Se<sub>3</sub>, Nat. Phys. 12, 852 (2016).
- [10] L. Fu and E. Berg, Odd-parity topological superconductors: Theory and application to Cu<sub>x</sub>Bi<sub>2</sub>Se<sub>3</sub>. Phys. Rev. Lett. 105, 097001(R) (2010).
- [11] M. Sato, Topological odd-parity superconductors. Phys. Rev. B 81, 220504 (2010).
- [12] D. A. Ivanov, Non-Abelian statistics of half-quantum vortices in p-wave superconductors, Phys. Rev. Lett. 86, 268 (2001).
- [13] X.-L. Qi and S.-C. Zhang, Topological insulators and superconductors, Rev. Mod. Phys. 83, 1057 (2011).
- [14] A. Y. Kitaev, Unpaired Majorana fermions in quantum wires. Phys. Usp. 44, 131 (2001).
- [15] M. Leijnse and K. Flensberg, Introduction to topological superconductivity and Majorana fermions, Semicond. Sci. Technol. 27, 124003 (2012).
- [16] J. F. Venderbos, V. Kozii, and L. Fu, Odd-parity superconductors with two-component order parameters: Nematic and chiral, full gap, and Majorana node, Phys. Rev. B 94, 180504(R) (2016).
- [17] M. Hecker and R. M. Fernandes, Phonon-induced rotation of the electronic nematic director in superconducting Bi<sub>2</sub>Se<sub>3</sub>, Phys. Rev. B **105**, 174504 (2022).
- [18] M. Yokoyama, H. Nishigaki, S. Ogawa, S. Nita, H. Shiokawa, K. Matano, and G. Q. Zheng, Manipulating the nematic director by magnetic fields in the spin-triplet superconducting state of Cu<sub>x</sub>Bi<sub>2</sub>Se<sub>3</sub>, Phys. Rev. B 107, L100505 (2023).
- [19] C.-w. Cho, J. Shen, J. Lyu, O. Atanov, Q. Chen, S. H. Lee, Y. S. Hor, D. J. Gawryluk, E. Pomjakushina, M. Bartkowiak, M. Hecker, J. Schmalian, and R. Lortz,

- Z3-vestigial nematic order due to superconducting fluctuations in the doped topological insulators Nb<sub>x</sub>Bi<sub>2</sub>Se<sub>3</sub> and Cu<sub>x</sub>Bi<sub>2</sub>Se<sub>3</sub>, Nat. Commun. 11, 3056 (2020).
- [20] M. P. Smylie, Z. Islam, A. Glatz, G. D. Gu, J. A. Schneeloch, R. D. Zhong, S. Rosenkranz, W.- K. Kwok, and U. Welp, Multimodal synchrotron x-ray diffraction across the superconducting transition of Sr<sub>0.10</sub>Bi<sub>2</sub>Se<sub>3</sub>, Phys. Rev. B 110, 024509 (2024).
- [21] S. Zhou and Z. Wang, Chern Fermipocket, topological pair density wave, and charge-4e and charge-6e superconductivity in kagome superconductors, Nat. Commun. 13, 7288 (2022).
- [22] R. M. Fernandes and L. Fu, Charge-4e superconductivity from multicomponent nematic pairing: Application to twisted bilayer grapheme, Phys. Rev. Lett. **127**, 047001 (2021).
- [23] I. Shipulin, N. Stegani, I. Maccari, K. Kihou, C.-H. Lee, Q. Hu, Y. Zheng, F. Yang, Y. Li, C.-M. Yim, R. Hühne, H.-H. Klauss, F. Caglieris, E. Babaev, M. Putti, and V. Grinenko, Calorimetric evidence for two phase transitions in Ba<sub>1-x</sub>K<sub>x</sub>Fe<sub>2</sub>As<sub>2</sub> with fermion pairing and quadrupling states, Nat. Commun. 14, 6734 (2023).
- [24] T. Kawai, C. G. Wang, Y. Kandori, Y. Honoki, K. Matano, T. Kambe, and G.-q. Zheng, Direction and symmetry transition of the vector order parameter in topological superconductors Cu<sub>x</sub>Bi<sub>2</sub>Se<sub>3</sub>, Nat. Commun. 11, 235 (2020).
- [25] M. Kriener, K. Segawa, Z. Ren, S. Sasaki, S. Wada, S. Kuwabata, and Y. Ando, Electrochemical synthesis and superconducting phase diagram of Cu<sub>x</sub>Bi<sub>2</sub>Se<sub>3</sub>, Phys. Rev. B 84, 054513 (2011).
- [26] See Supplemental Material at http://link.aps.org/supplemental/10.1103/ddvn-8c9n for c-axis distortion and its disappearance under a magnetic field above  $H_{c2}$ .
- [27] M. Hecker and J. Schmalian, Vestigial nematic order and superconductivity in the doped topological insulator Cu<sub>x</sub>Bi<sub>2</sub>Se<sub>3</sub>, npj Quantum Mater. **3**, 26 (2018).
- [28] Y. Sun, S. Kittaka, T. Sakakibara, K. Machida, J. Wang, J. Wen, X. Xing, Z. Shi, and T. Tamegai, Quasiparticle evidence for the nematic state above T<sub>c</sub> in Sr<sub>x</sub>Bi<sub>2</sub>Se<sub>3</sub>, Phys. Rev. Lett. 123, 027002 (2019).
- [29] A. Larkin and A. Varlamov, Theory of Fluctuations in Superconductors (Oxford University Press, New York, 2005)
- [30] E. Lahoud, E. Maniv, M. S. Petrushevsky, M. Naamneh, A. Ribak, S. Wiedmann, L. Petaccia, Z. Salman, K. B. Chashka, Y. Dagan, and A. Kanigel, Evolution of the Fermi surface of a doped topological insulator with carrier concentration, Phys. Rev. B 88, 195107 (2013).